# Nanoscale

Accepted Manuscript


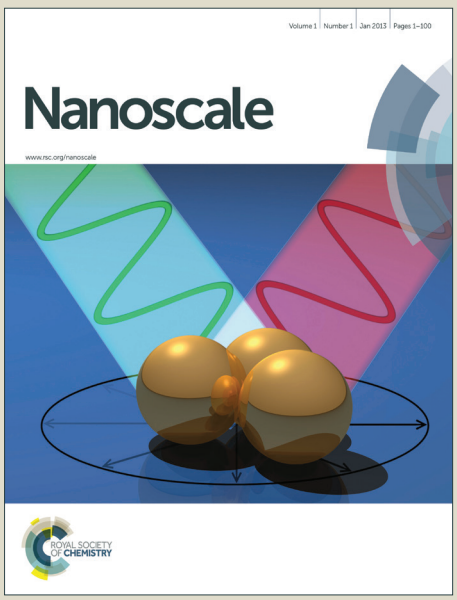





ROYAL SOCIETY OF CHEMISTRY

www.rsc.org/nanoscale

# Topical Gene Silencing by iontophoretic delivery of antisense oligonucleotide-dendrimer nanocomplex: Proof of concept in a skin cancer mouse model

Venkata Vamsi K. Venuganti[1,3], Manju Saraswathy[1], Chandradhar Dwivedi[1], Radhey S. Kaushik[2], Omathanu P. Perumal[1*]

[1]Department of Pharmaceutical Sciences, College of Pharmacy, South Dakota State University, Brookings, SD 57007, USA.

[2]Department of Biological and Microbiology, College of Agriculture and Biological Sciences, South Dakota State University, Brookings, SD 57007, USA.

[3]Current Address: Department of Pharmacy, Birla Institute of Technology, Hyderabad Campus, Shameerpet, Andhra Pradesh 500078, India.

*Corresponding Author: Omathanu Perumal

Email: omathanu.perumal@sdstate.edu

Ph: 001-605-688-4745

**Abstract**

The study was aimed at investigating the feasibility of using poly (amidoamine) (PAMAM) dendrimer as a carrier for topical iontophoretic delivery of antisense oligonucleotide (ASO). Bcl-2, an anti-apoptotic protein implicated in skin cancer was used as a model target protein to demonstrate the topical gene silencing approach. Confocal laser scanning microscopy studies demonstrated that iontophoretically delivered ASO-dendrimer complex can reach the viable epidermis in porcine skin. In contrast, passively delivered free or dendrimer complexed ASO was mainly localized to the stratum corneum. The cell uptake of ASO was significantly enhanced by the dendrimer complex and the complex suppressed Bcl-2 levels in the cell. In skin cancer mouse model, iontophoretically delivered ASO-dendrimer complex reduced tumor volume by 45% and was consistent with the reduction of Bcl-2 protein levels. The iontophoretically delivered ASO-dendrimer complex caused significant apoptosis in skin tumor. Overall, the findings from this study demonstrate that dendrimer is a promising nanocarrrier for developing topical gene silencing approaches for skin diseases.

**Keywords**: Antisense oligonucleotide, PAMAM dendrimer, bcl-2 protein, nanocarrier, iontophoresis, topical delivery, gene silencing

## Introduction

Gene silencing is an effective strategy to limit the disease progression by inhibiting the expression of the target protein. This can be achieved using antisense oligonucleotides (ASO), ribozymes or small interference RNA (siRNA). ASO is a short single strand of 10-22 nucleotides that hybridizes with DNA or mRNA to cause transcriptional or translational arrest respectively.[1] ASO forms Watson-Crick base pairs with target mRNA to inhibit ribosomal entry and the ASO-mRNA duplex is degraded by RNase-H enzyme.[1-3]

Skin due to its easy accessibility, is an attractive target for developing gene-silencing strategies for the treatment of localized skin diseases including skin cancer, psoriasis, atopic dermatitis among others.[4-7] Topical anti-sense therapy can be confined to the affected area and thus reducing the likelihood of systemic effects. Further, skin has relatively less nucleases compared to other routes of delivery.[8] However, the high molecular weight and negative charge of ASO limits its effective delivery through skin. Further, the delivery of ASO is limited by poor cell uptake and ability to escape the harsh endo-lysosomal compartment in the cell.[9] The systemic half-life of ASO ranges from few minutes to hours due to rapid degradation by nucleases.[10] Although, the stability of ASO can be improved by chemical modifications to phosphate backbone, the membrane permeability still remains a challenge.[11,12] Taken together, there is a need to develop efficient carriers to improve the membrane permeability and cell uptake of ASO.

To this end, various enhancement techniques have been studied to increase the skin penetration of ASO.[13] Chemical enhancers and skin penetrating peptides have been shown to enhance the skin penetration of ASO and siRNA.[14,15] Physical enhancement techniques including electroporation, low frequency ultrasound, laser ablation and microneedles have been investigated for the delivery of ASO.[16-19] Iontophoresis is a non-invasive physical enhancement method that uses a small electric current (≤0.5mA/sq.cm) to transport charged molecules through the skin.[20] The iontophoretic delivery is influenced by physicochemical properties of the molecule including

pH, charge, ionic strength and size of the molecule in addition to current strength and duration of current application.[20]

Cathodal iontophoresis has been studied for the delivery of oligonucleotides through skin, and the skin penetration was found to be strongly influenced by the nucleic acid composition of the oligonucleotides.[13, 21, 22] Sakamoto et al[6] have shown that therapeutic levels of ASO interlukin-10 can be delivered by iontophoresis *in vivo* in a mouse model of atopic dermatitis. However, most of the ASO was retained in the SC. In a comparative study between electroporation and iontophoresis, Regnier and Preat[23] reported that both techniques achieved comparable ASO levels in the skin, but cell and nuclear uptake of ASO was observed only with electroporation. Electroporation uses very high voltage pulses (100 V) to create pores for the transport of molecules through skin. On the other hand, in iontophoresis the molecules are mainly transported through follicular routes and existing pores in the skin.[20, 24] Taken together, these studies suggest the need for using suitable carriers to improve the iontophoretic delivery of nucleic acid.

Cationic polymers and cationic liposomes have been shown to be effective in improving the cell uptake of ASO *in-vitro* and *in-vivo*.[25-27]. However there are limited studies on the use of cationic carriers for ASO delivery through skin.[7, 28] Brus et al[28] demonstrated the use of polyethyleneimine (PEI) for iontophoretic delivery of oligonucleotide through skin. Here, we report for the first time the use of dendrimer for iontophoretic delivery of ASO. Dendrimer is a branched polymer with core-shell architecture.[29] The dendrimer offers a number of advantages over other polymers. Dendrimer is a well-defined monodisperse spherical polymer with a high density of surface functional groups.[29] More importantly, the number and type of surface functional groups can be easily altered by choosing an appropriate dendrimer generation. The high density of surface functional groups in the dendrimer can be used for complexation of ASO and at the same time the surface functional groups also can aid in the iontophoretic delivery of the complex. Although dendrimers have been investigated for gene delivery by various routes[30], there is hardly any study on its use for topical delivery of ASO through skin. Earlier, we have reported the structure-permeability of dendrimers.[31]

Given the high negative charge of the ASO, there is limited iontophoretic transport of ASO through the skin, which is negatively charged at physiological pH. [21, 22, 32] On the other hand, the cationic dendrimer can effectively condense the ASO resulting in a net positively charged complex, which can then be delivered by anodal iontophoresis. Further, the dendrimer can enhance the cell uptake and inside the cells, the high density of surface amine groups in the dendrimer can also aid in the endo-lysosomal escape of ASO.[30] Based on this hypothesis, the goal of this proof-of-concept study is to test the feasibility of using dendrimer for iontophoretic delivery of ASO using Bcl-2 as a model target gene. B-cell lymphoma/leukemia 2 (Bcl-2) is an anti-apoptotic protein that belongs to a multi-gene family of cell apoptosis regulatory proteins.[33] The overexpression of Bcl-2 has been implicated in tumor progression and resistance to chemotherapeutic agents in various types of cancers including skin cancer.[33,34]

## Experimental

### Chemicals

Human Bcl-2 ASO (5'-TCTCCCAGCGTGCGCCAT-3') and its corresponding sense oligonucleotide was used for in-vitro studies, while mouse Bcl-2 ASO (5'-TCTCCCGGCTTGCGCCAT-3') and its corresponding sense oligonucleotide was used for *in vivo* studies in mice. Phosphorothioate ASOs including fluorescent labeled ASO were purchased from Midland Certified Reagent Company, Midland, TX. ASO was labeled with fluoroisothiocynate (FITC) or rhodamine at the 5'end. Generation 4 polyamidoamine (PAMAM) dendrimer ($G_4$-$NH_2$; MW: 14,290 Da) was purchased from Dendritech Inc., Midland, MI. FITC, 7,12-dimethyl benzanthracene (DMBA), 12-O-tetradecanoylphorbol 13-acetate (TPA), N-hydroxyethylpiperazine-N'-2-ethanesulfonic acid (HEPES), Tris-borate EDTA (TBE) buffer components, EDTA disodium salt, sodium chloride, sodium dodecyl sulfate (SDS), triton X-100, sucrose, leupeptin, pepstatin and phenylmethanesulphonylfluoride (PMSF) were purchased from Sigma-Aldrich Chemical Co., St. Louis, MO. Dulbecco's modified Eagle's medium (DMEM), fetal bovine serum (FBS), trypsin EDTA and phosphate buffered saline (PBS) were from Mediatech Inc., Manassas, VA. Apoptosis assay kit was obtained from Roche Diagnostics, Indianapolis, IN. Primary antibodies and horseradish peroxidase conjugated goat anti-mouse secondary antibodies were purchased from Santa Cruz biotechnology Inc., Santa Cruz, CA. All the buffers were prepared using Milli-Q water with 18.2 MΩ resistivity (Barnstead, Madison, WI).

### Preparation and characterization of ASO-dendrimer complex

Bcl-2 ASO (5.6 kDa) with a phosphorothioate backbone was used in this study. The $G_4$-$NH_2$ dendrimer was mixed with ASO in HEPES buffer (pH 7.4) and incubated at room temperature for 1 hr. The complex was prepared with different nitrogen to phosphate (N/P) ratios including 10:1, 1:1 and 1:10. For co-localization studies, $G_4$-$NH_2$ dendrimer was labeled with FITC.[31] Briefly, FITC (5 mg/mL) was dissolved in acetone and slowly added to the dendrimer in phosphate-buffered saline (PBS; pH 7.4) and incubated at room temperature for 24 hrs. Free FITC was separated by dialysis (nitrocellulose membrane, Mwt cutoff 1–10 kDa; Spectrum laboratories

Inc., Rancho Dominguez, CA). The conjugate was further purified using a Sephadex PD10 column (Amersham biosciences, Piscataway, NJ). The FITC labeled dendrimer was lyophilized and stored at 4$^{o}$C. The dendrimer-FITC conjugate was characterized using NMR and UV spectroscopy.[31]

**Characterization of ASO-dendrimer complex**

The hydrodynamic size and zeta potential of the ASO-dendrimer complex was determined by dynamic light scattering (DLS) using ZetaSizer Nano ZS, (Malvern Instrument Westborough, MA) at a concentration of 0.01 mg/ml. Polyacrylamide gel electrophoresis (PAGE) was used to confirm the complexation of ASO to dendrimer. ASO-dendrimer complexes were analyzed using 20% w/w PAGE under non-denaturing conditions and 1 µM equivalent of ASO was loaded onto the gel. Electrophoresis was conducted at 100 V for 40 min and bromophenol blue was used as a marker. TBE buffer (0.89M Tris base 0.89 M; 0.89M boric acid and 0.02M EDTA) was used for gel electrophoresis. To further confirm the complex formation, in a separate experiment, ASO-dendrimer complex was incubated with dextran sulfate for 4 hrs to study the dissociation of free ASO. Later, the samples were analyzed by gel electrophoresis. After electrophoresis, the gel was incubated with SYBR Gold stain for 30 min at room temperature. The gel was washed in deionized water and visualized using a gel documentation system (Biochemi II, UVP laboratory products, Upland, CA).

**In-vitro Skin penetration studies**

In-vitro skin penetration studies was conducted using porcine skin. Porcine ears were procured from the Department of Animal Sciences at South Dakota State University. The ears were washed under tap water and dorsal hair was removed using a hair clipper (Golden A5, Oster, Niles, IL). Later, the skin was excised from the ear. The excised skin was dermatomed to a thickness of 300 µm using an electric dermatome (Padgett Instruments, St. Louis, MO). The dermatomed skin was washed and used for skin penetration studies. The skin was sandwiched between the donor and receptor chambers of a vertical Franz diffusion cell (PermeGear, Inc., PA) with the SC facing the donor chamber. Phosphate buffered saline (PBS, pH 7.4) with 0.05% (w/v) sodium azide was used as the receptor medium (6 mL) and the temperature was maintained at 37

$^{o}$C by circulating heated water. The skin area exposed to the donor chamber was 0.64 sq.cm and the receptor phase was stirred using a magnetic stir bar. To ensure that the skin was intact, transepidermal water loss (TEWL) (Vapometer, Delfin, Kuopio, Finland) and skin resistance were measured.[31] Only skin samples which had a TEWL <10 g/m$^2$/h and a resistance >20 kΩ/cm$^2$ were used in the study.

Donor chamber was loaded with 0.2 mL of 15 μM of free ASO or dendrimer-ASO complex. Skin penetration was studied in the presence and absence of 0.3 mA/cm$^2$ electric current (Phoresor II, Iomed, Salt Lake City, UT) for 4 hrs. Ag/AgCl electrode (In-vivo metric, Healdsburg, CA) was used for iontophoresis. Anode (Ag) was placed in the donor chamber for the delivery of ASO-dendrimer complex, while for free ASO, cathode (AgCl) was placed in the donor chamber. To prevent the direct contact of electrodes with ASO, a salt bridge (0.2mM sodium chloride in agarose gel) was used. At the end of the study, the skin was washed with PBS and mounted on a glass slide for analysis by confocal laser scanning microscopy.

**Confocal laser scanning microscopy (CLSM)**

For CLSM studies, the skin was placed with the *stratum corneum* (SC) facing the confocal microscope (Fluoview FV300, Olympus ix70, Olympus, Center Valley, PA). FITC was excited using Argon laser at an excitation wavelength of 488 nm. The images were observed using Plan-neofluor 40/0.85 objective. Optical sections of the skin were obtained in xyz and xz planes with z-axis being perpendicular to the skin surface (xy). [31] To study the depth of penetration, xyz images were generated by scanning the skin from the surface (z = 0 μm) to 100 μm at a step size of 5 μm/scan. To generate the xz sections, a horizontal line was "drawn" across the region of interest in the z = 0 μm in xy plane and then optically sliced through the image of successive xy-sections to generate xz planar optical cross-sections. For xz sections, the images were optically sectioned from the surface of the skin (z = 0 μm) to 100 μm depth at a step size of 1 μm/scan.[31] All images were obtained with the same optical aperture, lens and scan speed setting. Blank skin did not show any autofluorescence under the experimental conditions. To quantify the skin penetration, FITC labeled ASO was used. For co-localization studies, the dendrimer was labeled with FITC and ASO was labeled with rhodamine (Midland certified reagent company, Midland, TX). After treatment

with ASO-dendrimer complex, the skin was analyzed CLSM. FITC was excited by Argon laser at 488 nm wave length and rhodamine was excited by Helium-Neon (HeNe) laser at 543 nm wavelength.

**Image Analysis**

For image analysis, optical sections (xyz) were analyzed using Fluoview software (Olympus, Center Valley, PA). The dendrimer distribution within the confocal images was quantified by integrating the fluorescence pixel intensity.[31] Three to four regions were analyzed for each skin sample and the measurements were repeated in three to four skin samples. The thickness of porcine SC was considered to be 20 μm based on our previous studies.[31] The fluorescence pixels of the xz images was measured both in the SC (0-20μm) and in the viable epidermis (VE, 20-100μm). Since the target site is viable epidermis, the percent pixels in the viable epidermis (20–100 μm) was calculated using the following formula:

$$\%\ Pixel\ Intensity\ in\ viable\ epidermis = \frac{Total\ Pixel\ intensity\ in\ VE\ (20-100\mu m)}{Total\ Pixel\ Intensity\ in\ skin\ (0-100\mu m)}$$

Overlap coefficient was calculated from the acquired images using ImageJ software (NIH, Frederick, MD).

**Cell-uptake studies**

To determine the cell uptake of ASO-dendrimer complex, A431, human epidermoid carcinoma cells were used (American Type Culture Collection, Manassas, VA). A431 cells were grown in DMEM supplemented with 10% heat inactivated FBS and 100 units/mL of penicillin and streptomycin. Cells ($1x10^5$) were plated in culture dish and maintained at 37 $^oC$ in an incubator with 5% $CO_2$. After 24 hrs, the cells were incubated with free or dendrimer complexed ASO (FITC labeled; 1 μM) in serum free medium (DMEM). Cells were treated for 15, 30, 60 and 120 min at 37 $^oC$ in an incubator with 5% $CO_2$. After treatment, the cells were washed with ice cold PBS. The cells were centrifuged to form a pellet which was then resuspended in PBS. The cells (5,000

counts) were analyzed in a flow cytometer (FACS Scan, BD biosciences, San Jose, CA) for fluorescence intensity from FITC labeled ASO.

**In vivo studies in skin cancer mouse model**

The animal studies were performed after approval from the institutional animal care and use committee (IACUC) at South Dakota State University. Female CD1 mice (Charles River Laboratories, Wilmington, MA) were randomly divided into eight groups (Table S1 in supporting information) with 4 to 5 mice in each group. The animals had free access to food and water. The skin tumor was initiated by topical application of 7, 12-dimethyl benzanthracene (DMBA, 200 nmol/100 µL in acetone) followed by application of tumor promoter, 12-O-tetradecanoylphorbol 13-acetate (TPA; 5 nmol/100 µL in acetone) twice a week for 16 weeks.[35]

The animals were anesthetized using isoflurane in 0.5 to 1% in oxygen for 2 hrs (Vetequip Inc., Pleasanton, CA). Treatment was started at the 20$^{th}$ week after tumor initiation. A single tumor was selected in the most accessible region of the mouse for topical treatment. Four doses of 90 µg of ASO or ASO-dendrimer complex was applied on days 1, 3, 5 and 7. In control group, ASO or ASO-dendrimer complex was injected intradermally at the base of the tumor. The sense oligonucleotide-dendrimer complex (negative control) was injected intradermally to test for non-specific gene silencing effects. Free ASO or ASO-dendrimer complex was mixed with 0.3% agarose gel with 2 mM of sodium chloride and was used for topical treatment studies. In the topical control group, just 0.3% agarose and 2 mM of sodium chloride were used. For iontophoretic studies, the delivery electrode was placed in the ASO/ASO-dendrimer complex gel, while the other electrode was placed in blank agarose gel separated by a distance of at least 2 cm. A salt bridge was used to prevent the direct contact between the electrode and the formulation. A current density of 0.5 mA/cm$^2$ was applied for 2 hrs under isoflurane anesthesia. Figure 1 shows the set-up for *in vivo* iontophoretic studies. Anodal iontophoresis was used for the delivery of ASO-dendrimer complex and cathodal iontophoresis was used for the delivery free ASO. For passive delivery, the ASO/ASO-dendrimer complex gel was applied on the tumor for 2 hrs without any current application. The skin tumor length ($l$), breadth ($b$) and height ($h$) were measured using a vernier caliper and the volume was calculated using the equation $V = l.b.h.$[36] Tumor volume was measured

on days 0, 1, 3, 5 and 7. The percent reduction in tumor volume at the end of 7-day treatment was calculated using the following equation:

$$\frac{tumor\ volume\ after\ treatment}{tumor\ volume\ before\ starting\ \ treatment} \times 100$$

**Apoptosis assay**

The skin tumor was sectioned (8 µm thickness) in a cryomicrotome and terminal deoxynucleotidyl transferase dUTP Nick end Labeling (TUNEL) assay was performed using a commercial apoptosis kit (Roche biosciences, Indianapolis, IN). The tissue section was placed on a hot plate at 30$^{o}$C overnight. The tissue section was fixed with acetone for 5 min and then air dried for 30 min. To block non-specific binding, the sample was incubated with 1% goat serum for 20 min at room temperature. For positive control, the skin section from a normal mouse was treated with DNase I for 10 min at 37 $^{o}$C to induce nicks in the DNA. Later, the tissue sections were incubated with freshly prepared mixture of fluorescein labeled deoxyuridine triphosphate (dUTP) and nucleotidyl transferase for 1 hr at 37$^{o}$C. Then, the samples were washed three times with PBS (5 min each). The sample was counter stained with propidium iodide (1 µg/mL) for 10 min at room temperature and washed with PBS. The sample was air dried for 1 hr and mounted on a glass slide using cytoseal. The slide was visualized in a fluorescence microscope.

**Protein analysis**

At the end of the treatment, mouse was euthanized and the treated area was excised. For protein extraction, the tissue was dispersed in Tris HCl buffer (pH 7.0) and homogenized in a tissue homogenizer. The skin homogenate was filtered and centrifuged at 10,000 rpm at 4$^{o}$C for 1 hr. The cell membrane was lysed by passing through a 30G syringe and the lysate was centrifuged at

10,000 rpm for 20 min in cell lysis buffer. The supernatant was collected and was stored at -20$^{o}$C till further analysis. Bcl-2 and β-actin protein levels were determined using Western blot.

SDS-PAGE was performed to separate the protein using 12.5% acrylamide gel. Electrophoresis was carried out at 90 V for 4 hrs in Laemmli buffer. The proteins were transferred to a nitrocellulose membrane in transfer buffer under 40 V current application for 20 hrs at 4$^{o}$C. The membrane was then probed for Bcl-2 protein by incubating with Bcl-2 specific monoclonal antibody at 4°C. After washing the blot 3 times in TTBS (Tween 20, Tris buffered saline) for 10 min, the membrane was incubated for 1 hr with horseradish peroxidase–conjugated secondary antibody. The blot was washed in TTBS and treated with enhanced chemi-luminiscence reagent (ECL, Amersham biosciences, Piscataway, NJ) according to the manufacturer's instruction. The blot was imaged in a gel documentation system (Biochemi system II, UVP laboratory products, Upland, CA). The densitometric analysis of the bands were performed using Labworks software.

**Statistical analysis**

Results from the studies were presented as mean±standard deviation (n=3-5). The results were compared using one way analysis of variance (ANOVA) (Prism, Instat, CA) and the results were considered to be significant at $p < 0.05$.

## Results

### Characterization of ASO-dendrimer complex

Table 1 shows the particle size of dendrimer-ASO complexes at different N/P ratios. The particle size was determined using dynamic light scattering method. A small compact complex was formed at N/P ratio of 10:1, while the particle size was large when 1:1 and 1:10 N/P ratios were used. The polydispersity index which is a measure of particle size distribution was lowest with N/P ratio of 10:1 indicating the formation of a compact uniformly sized complex. The results were also confirmed using atomic force microscopy (AFM; Figure S1 in supporting information). The particle size determined by AFM was close to the particle size determined by dynamic light scattering method. A positive zeta potential was observed for the complex with 10:1 N/P ratio. On the other hand, the zeta potential was negative when a lower N/P ratio was used. The complex formation was confirmed by gel electrophoresis. SYBR gold intercalates only with free ASO and therefore, only free ASO band is visualized (Figure S2 in supporting information). The ASO-dendrimer complex was not electrophoresed and was retained in the sample well, while, free ASO migrated in polyacrylamide gel. The complex with N/P ratio of 10:1 showed complete complexation of ASO, while only partial complexation was found with N/P ratio of 1:1 (Fig. S1). To further confirm these result, the complexes were incubated with negatively charged dextran sulfate for 4 hrs. Dextran sulfate is negatively charged polysaccharide and therefore, competes with ASO to form a complex with the positively charged dendrimer. After incubation with dextran sulfate, free ASO bands were seen with all the complexes indicating the dissociation of ASO-dendrimer complex (Fig. S1). Taken together, the results confirm the formation of a positively charged compact dendrimer-ASO complex at 10:1 N/P ratio.

### In vitro skin penetration of ASO-dendrimer complex

CLSM was used to characterize the depth and extent of penetration of ASO and ASO-dendrimer complex. FITC labeled ASO was used for quantifying the skin penetration. The representative xz and xyz images of skin treated with ASO/ASO-dendrimer complex is shown in Figure 2 and Figure S3 (see supporting information) respectively. The extent of ASO penetration

into viable epidermis was quantified from the ratio of the pixels in the optical skin sections from 20 to 100 µm (viable epidermis) to the total pixels from 0-100 µm cumulative images.

The passively delivered free ASO was mainly localized to SC (20 µm) with less than 6% of fluorescence in the viable epidermis (Fig. 2, Fig. S3 and Table 2). Although, ASO-dendrimer complex showed higher skin penetration compared to free ASO, the difference was not statistically significant (Table 2). Cathodal iontophoresis increased skin penetration of free ASO compared to passive delivery. However, the extent of skin penetration was not significantly different (Table 2). On the other hand, anodal iontophoresis of ASO-dendrimer complex showed significant skin penetration upto 100 µm in the viable epidermis (Fig. 2, Fig. S3). Anodal iontophoresis of ASO-dendrimer complex enhanced the skin penetration of ASO complex by 5-fold compared to passive delivery of ASO and 3-fold compared to iontophoretic delivery of free ASO (Table 2).

To test if the complex was transported intact through the skin, co-localization studies were carried out using rhodamine labeled ASO and FITC labeled dendrimer. Figure 3 shows the cumulative xyz images from 0 to 100µm after passive and iontophoretic delivery of ASO-dendrimer complex. The overlay images show that the majority of ASO was complexed to dendrimer in the skin. Overlap coefficient determined from image analysis was 0.72 and 0.69 for passive and iontophoretic delivery of ASO-dendrimer complex, respectively. The overlap coefficient values indicates that more than 70% of the ASO was transported as a complex with the dendrimer. In case of iontophoresis, a significant amount of the complex was transported to the viable epidermis.

**Cell uptake of ASO-dendrimer complex**

To determine whether the dendrimer can enhance the cell uptake of ASO, studies were conducted in A431 human epidermoid carcinoma cells using flow cytometry. As shown in Figure 4, there was a significant shift in the fluorescence intensity of FITC labeled ASO after treatment with ASO-dendrimer complex and the complex was taken up within 15 minutes. On the other hand, there was limited cell uptake of free ASO even after 2 hrs.

To confirm if enhanced cell uptake resulted in better gene-silencing effect, the levels of Bcl-2 was measured by Western blot. The ASO-dendrimer complex decreased Bcl-2 expression by 46% compared to 20% after treatment with free ASO (Fig. S4, Supporting information). On the other hand, treatment with the negative control (sense oligonuceltoide-dendrimer complex) did not show any change in Bcl-2 levels, demonstrating that the gene silencing effect was specific to Bcl-2 ASO.

**In vivo efficacy studies**

Skin tumors were initiated using DMBA and promoted by the TPA application in mouse for 16 weeks. The average weight of mice steadily increased up to 14 weeks and was stable thereafter (Fig. S5, supporting information). Tumors started to appear seven weeks after DMBA application and tumor volume as well as tumor number increased every week. There was 100% tumor incidence and the average number of papillomas was 14.3 per mouse 16 weeks after tumor initiation (Fig. S5, supporting information).

The tumor volume was measured before and at the end of seven-day treatment. Iontophoresis of free ASO did not show any reduction in tumor volume (Fig. S6, supporting information). On the other hand, iontophoretic delivery of ASO-dendrimer complex resulted in a gradual reduction in tumor volume with treatment (Fig. S6, supporting information). Figure 5 shows the percent decrease in tumor volume at the end of 7-day treatment compared to the initial tumor volume. The intradermal administration of ASO-dendrimer complex showed 20% reduction in tumor volume (Fig. 5). A similar reduction in tumor volume was also observed with iontophoretically delivered free ASO and passively delivered ASO-dendrimer complex (Fig. 5). On the other hand, iontophoretic delivery of ASO-dendrimer complex showed 45% reduction in tumor volume. The intradermal injection or topical application of free ASO did not show any significant decrease in tumor volume and was similar to saline treated group. As expected, treatment with a control sense sequence also did not show significant reduction in tumor volume (Fig. 5).

To determine the *in vivo* gene silencing effect, the expression of Bcl-2 in the skin tumor was measured by Western blot. There was <20% reduction in Bcl-2 protein expression after intradermal injection of ASO-dendrimer complex, passive delivery of ASO-dendrimer complex and iontophoresis of free ASO. On the other hand, there was a significant reduction in Bcl-2 levels (by 45%) after iontophoretic delivery of ASO-dendrimer complex (Fig. 6). There was no significant suppression of Bcl-2 levels with other treatment groups.

TUNEL assay was used to determine the cell apoptosis caused by Bcl-2 suppression. In Figure 7, the green fluorescence is from dUTP and red fluorescence is indicative of nuclear staining with propidium iodide. Iontophoresis of ASO-dendrimer complex induced significant apoptosis in the basal layer of epidermis and cells surrounding the hair follicles (Fig. 7). On the other hand, there was no significant apoptosis after iontophoretic delivery of free ASO. Similarly, there was no fluorescence observed in the negative control, but as expected there was significant apoptosis in the positive control (sample treated with DNase I). Since the passive delivery of ASO or ASO-dendrimer complex did not show any significant reduction in Bcl-2 levels, the apoptosis assay was not performed for those treatment groups.

## Discussion

Our study was focused on investigating the feasibility of using dendrimer as a nanocarrier for iontophoretic delivery of anti-sense oligonculeotide for topical gene silencing. This study builds on our earlier findings, where we reported the structure-skin permeability of PAMAM dendrimers by passive and iontophoretic transport.[31] Skin penetration of dendrimer was found to be strongly dependent on the charge and the molecular size of dendrimers. In particular, the cationic dendrimer interacted with the skin lipids resulting in higher skin penetration.[37] Iontophoresis was found to increase the skin transport of cationic dendrimers by follicular and non-follicular routes.[31] Given the core-shell architecture and high surface charge density of dendrimers, it showed higher skin penetration compared to other cationic polymers (PEI) and cationic liposomes.[38]

Similar to our studies, CLSM has been used to quantify the transport of molecules through skin.[28,39] We have earlier found that results from CLSM studies correlated well with spectrofluorimetry.[31] Based on our earlier results from tape-stripping studies, we defined the viable epidermis to be 20-100 μm.[31] Since the quantitation beyond 100μm in the skin can be limited by the fluorescence quenching by the tissue[28], the imaging depth was limited to100μm.[28] The complexation of ASO by dendrimer increased the skin transport by condensing the ASO and reducing its negative charge. Although, the complex resulted in better skin penetration compared to free ASO, there was limited penetration into the viable epidermis. Iontophoresis increased both the depth and extent of skin penetration of ASO-dendrimer complex.

Unlike other physical enhancement methods, iontophoresis is a non-invasive technique, since it mainly acts on the molecule rather than the skin barrier.[19] Iontophoreis enhances skin penetration by electromigration from the delivery electrode. Since the skin is negatively charged at physiological pH[33], cations are better candidates for iontophoretic delivery. This is because the skin's permeslectivity to cations gives rise to electroosmosis from anode to cathode during iontophoresis.[32] Therefore, the anodal delivery of net positively charged ASO-dendrimer complex can benefit from the combined influence of electrorepulsion and electroosmosis.[20] In contrast, the cathodal delivery of ASO is limited by negative charge of the skin and opposing electroosmotic flow from anode to cathode.[20] The strong binding of free ASO to SC can also limit the transport

to deeper skin layers.[21, 22] Although, electromigration is the predominant transport mechanism in iontophoresis, electroosmosis is especially important for the transport of large molecules.[40] Our skin penetration results are consistent with the studies reported by Brus et al[28] with free and PEI complexed oligonucleotide in human skin. The porcine skin used in our study is morphologically and functionally similar to human skin.[41] The core-shell architecture of the dendrimer can result in better skin penetration than PEI.[38]

ASO-dendrimer complex was found to remain stable during transport as evidenced from co-localization studies. It is important for the complex to remain intact for uptake by the target cells in the skin. The cell uptake mechanism and endo-lysmotropic effects of dendrimer-ASO complex is well documented.[26, 30, 42] The ASO-dendrimer complex is taken up in the cells by endocytosis. Once endocytosed into the cell, the complex is transported through the endo-lysosomal pathway before reaching the cytoplasm and nucleus. [26, 42] The high density of surface amine groups in the dendrimer can act as a proton sponge in the endosomal compartment leading to osmotic swelling and release of the complex from the endosomes into the cytoplasm. [26, 30, 42] Taken together, this resulted in significantly higher suppression of Bcl-2 levels in the target cells.

Bcl-2 is a cell survival protein that regulates the intrinsic apoptosis pathway and therefore the suppression of Bcl-2 leads to apoptosis induced cell death.[33] Bcl-2 exerts its anti-apoptotic functions by blocking cytochrome-c release from the mitochondria, which plays an important role in initiating caspase activated apoptosis.[43] In normal skin, Bcl-2 protein is expressed mainly in the basal layers.[43] Bcl-2 is normally down regulated in suprabasal layers, but patients with pre-tumorigenic conditions such as actinic keratosis have high levels of Bcl-2 which leads to the development of squamous cell carcinoma (SCC).[44] In case of basal cell carcinoma (BCC), up regulation of Bcl-2 leads to extended cell survival and resistance to chemotherapy.[43] Bcl-2 ASO has been studied in several types of cancers including skin cancer. [33] Jansen et al[45] showed that Bcl-2 ASO (delivered using an implanted osmotic pump) along with chemotherapy resulted in complete tumor ablation in 80% of mice with established human melanomas. However, the systemic administration of Bcl-2 ASO has been reported to cause adverse effects due to its off-target binding in other tissues.[45] At higher doses (50 mg/kg/day), Bcl-2 ASO was also found to cause severe myocardial and liver necrosis in mice.[45] In the present study, only 2.5mg/kg body

weight of Bcl-2 ASO was used for localized topical treatment of skin cancer. The chemical carcinogenesis model mimics the squamous and basal cell carcinoma in humans.[35, 46, 47] Given the close correlation between the percent suppression of Bcl-2 levels and the reduction in tumor volume, the anti-cancer effects can be attributed to the specific gene silencing achieved by topical delivery of ASO.

As opposed to the intradermal injection, the topical delivery can result in uniform distribution of ASO-dendrimer complex in the epidermis. Further the intradermal injection can also result in systemic uptake by the dermal blood vessels. Taken together, the topical delivery can result in better efficacy than intradermal injection. The findings are consistent with other studies reported in the literature.[48, 49] Recently Kigasawa et al[49] reported higher anti-tumor activity for iontophoretically delivered CpG oligonucleotide compared to s.c injection in a mouse melanoma model. In the present study, the ASO was delivered only to a single skin tumor as a proof of concept. This is consistent with the skin tumor lesions seen in a limited area of the skin in humans. The amount of ASO delivered can be altered by changing the current and/or area of application. The current <0.5mA/sq.cm) used for iontophoresis is well-tolerated in humans.[20] Further we and others have shown that the current level used in this study does not cause any significant skin irritation. [6, 31, 49] Taken together, the topical delivery of ASO-dendrimer complex is a feasible therapeutic strategy in humans. Overall, the findings show that dendrimer and iontophoresis can synergistically enhance the skin penetration and cell uptake of ASO leading to effective gene-silencing in skin diseases.

## Conclusions

The results show that dendrimer can be used as a charged carrier for iontophoretic delivery of ASO. Iontophoresis significantly enhanced the penetration of ASO-dendrimer complex into viable epidermis. ASO-dendrimer complex was found to be intact in the skin after iontophoretic delivery. The dendrimer protected the ASO and enhanced the cell uptake. Iontophoretic delivery of ASO-dendrimer complex significantly reduced the tumor volume and caused gene silencing *in vivo*. Overall the findings from this study can be used to develop topical gene silencing strategies for various skin diseases.

## Acknowledgements

We thank Kelly Bruns and Adam Rhode for providing porcine ears for *in vitro* studies. We also would like to thank Dr. Alan Young from the Department of Veterinary and Biomedical Sciences, who allowed us to use his Flow Cytometer for our studies. This work was supported by funding from Skin Cancer Foundation New York and Department of Pharmaceutical Sciences, South Dakota State University.

## References


1. Y. Rojanasakul, Antisense oligonucleotide therapeutics: drug delivery and targeting, *Adv. Drug Deliv. Rev.* 1996, 18, 115-131.
2. S.T. Crooke, Progress toward oligonucleotide therapeutics: pharmacodynamic properties, *FASEB J.* 1993, 7, 288-294.
3. C.A. Stein, Y.C. Cheng, Antisense oligonucleotide as therapeutic agent-is the bullet really magical? *Science* 1993, 261, 1004-1012.
4. C.J. Wraight, P.J. White, Antisense oligonucleotides in cutaneous therapy, *Pharmacol. Therapy* 2001, 90, 89-104.
5. S. Dokka, S.R. Cooper, S. Kelly, G.E. Hardee, J.G. Karras, Dermal delivery of topically applied oligonucleotides via follicular transport in mouse skin, *J. Invest. Dermatol.* 2005, 124, 971–975.
6. T. Sakamoto, E. Miyazaki, Y. Aramaki, H. Arima, M. Takahashi, Y. Kato, M. Koga, S. Tsuchiya, Improvement of dermatitis by iontophoretically delivered antisense oligonucleotides for interleukin-10 in NC/Nga mice, *Gene Therapy* 2004, 11, 317-324.
7. S.T. Kim, K.M. Lee, H.J. Park, S.E. Jin, W.S. Ahn, C.K. Kim, Topical delivery of interleukin-13 antisense oligonucleotides with cationic elastic liposome for the treatment of atopic dermatitis, *J. Gene Med.* 2009, 11, 26-37.
8. R.C. Mehta, K.K. Stecker, S.R. Cooper, M.V. Templin, Y.J. Tsai, T.P. Condon, C.F. Bennett, G.E. Hardee, Intercellular adhesion molecule-1 suppression in skin by topical delivery of antisense oligonucleotides, *J. Invest. Dermatol.* 2000, 115, 805-812.
9. C. Beltinger, H.U. Saragovi, R.M. Smith, L. LeSauteur, N. Shah, L. DeDionisio, L. Christensen, L. Raible, L. Jarett, A.M. Gewirtz, Binding uptake and intracellular trafficking of phosphorothioate modified oligodeoxynucleotides, *J. Clin. Invest.* 1995, 95, 1814-1823.
10. C. Leonetti, A. Biroccio, B. Benassi, A. Stringaro, A. Stoppacciaro, S.C. Semple, G. Zupi, Encapsulation of c-myc antisense oligodeoxynucleotides in lipid particles improves antitumoral efficacy in vivo in a human melanoma line, *Cancer Gene Therapy* 2001, 8, 459-468.

11. X. Chen, N. Dudgeon, L. Shen, J.H. Wang, Chemical modification of gene silencing oligonucleotides for drug discovery and development, *Drug Discov. Today* 2005, 10, 587-593.
12. E. Fattal, A. Bochot, State of the art and perspectives for the delivery of antisense oligonucleotides and siRNA by polymeric nanocarriers, *Int. J. Pharm.* 2008, 364, 237-248.
13. R.M. Brand, P.L. Iversen, Transdermal delivery of antisense compounds, *Adv. Drug Deliv. Rev.* 2000, 44, 51-57.
14. V. Arora, T.L. Hannah, P.L. Iversen, R.M. Brand, Transdermal use of phospharadiamidate morpholino oligomer AVI-4472 inhibits cytochrome P450 3A2 activity in male rats. *Pharm. Res.* 2002, 19, 1465-1470.
15. T. Hsu, S. Mitragotri, Delivery of siRNA and other macromolecules into skin and cells using a peptide enhancer, *Proc. Natl. Acad. Sci. USA* 2011, 108,15816–15821.
16. V. Regnier, N.D. Morre, A. Jadoul, V. Preat, Mechanism of a phosphorothioate oligonucleotide delivery by skin electroporation, *Int. J. Pharm.* 1999, 184, 147-156.
17. Tezel, S. Dokka, S. Kelly, G.E. Hardee, S. Mitragotri, Topical delivery of anti-sense oligonucleotides using low-frequency sonophoresis, *Pharm. Res.* 2004, 21, 2219-2225.
18. W. Lin, M. Cormier, A. Samiee, A. Griffin, B. Johnson, C.L. Teng, G.E. Hardee, P.E. Daddona, Transdermal delivery of antisense oligonucleotides with microprojection patch (Macroflux$^{R}$) technology, *Pharm. Res.* 2001, 18, 1789-1793.
19. W.R. Lee, S.C. Shen, C.R. Liu, C.L. Fang, C.H. Hu, J.Y. Fang, Erbium:YAG laser-mediated oligonucleotide and DNA delivery via the skin: an animal study, *J. Control. Release* 2006, 115, 344-353.
20. Y.N. Kalia, A. Naik, J. Garrison, R.H. Guy, Iontophoretic drug delivery, *Adv. Drug Deliv. Rev.* 2004, 56, 619–658.
21. K.R. Oldenburg, K.T. Vo, G.A. Smith, H.E. Selick, Iontophoretic delivery of oligonucleotides across full thickness hairless mouse skin, *J. Pharm. Sci.* 1995, 84, 915-921.
22. R.M. Brand, A. Wahl, P.L. Iverson, Effects of size and sequence on the iontophoretic delivery of oligonucleotides, *J. Pharm. Sci.* 1998, 87, 49-52.

23. V. Regnier, V. Preat, Localization of a FITC-labeled phosphorothioate oligodeoxynucleotide in the skin after topical delivery by iontophoresis and electroporation, *Pharm. Res.* 1998, 15, 1596-1602.
24. W.I. Higuchi, S.K. Li, A. H. Ganhem, H. Zhu, Y. Song. Mechanistic aspects of iontophoresis in human epidermal membrane. *J. Control. Release* 1999, 62, 13-23.
25. L. Zhu, Z. Ye, K. Cheng, D.D. Miller, R.I. Mahato, Site-specific delivery of oligonucleotides to hepatocytes after systemic administration, *Bioconjugate Chem.* 2008, 19, 290-298.
26. R.L. Juliano, Intracellular delivery of oligonucleotide conjugates and dendrimer complexes, *Ann. N. Y. Acad. Sci.* 2006, 1082, 18-26.
27. X. Zhao, F. Pan, C.M. Holt, A.L. Lewis, J.R. Lu, Controlled delivery of antisense oligonucleotides: a brief review of current strategies, *Expert Opin. Drug Deliv.* 2009, 6, 673-686.
28. C. Brus, P. Santi, P. Columbo, T. Kissel, Distribution and quantification of polyethylenimine oligodeoxynucleotide complexes in human skin after iontophoretic delivery using confocal scanning laser microscopy, *J. Control. Release* 2002, 84, 171-181.
29. R. Esfand, D.A. Tomalia, Poly(amidoamine) (PAMAM) dendrimers: From biomimicry to drug delivery and biomedical applications, *Drug Discov. Today* 2001, 6, 427-436.
30. C. Dufes, I.F. Uchegbu, A.G. Schatzlein, Dendrimers in gene delivery, *Adv. Drug Deliv. Rev.* 2005, 57, 2177-2202.
31. V.V. Venuganti, P. Sahdev, M. Hildreth, X. Guan, O. Perumal, Structure-skin permeability relationship of dendrimers, *Pharm. Res.* 2011, 28, 2246-2260.
32. R. R. Burnette, B. Ongpipattanaku, Characterization of permeslective properties of skin. *J. Pharm. Sci.* 1987, 76, 765-773.
33. R.J. Klasa, D.M. Gillum, R.E. Klem, S.R. Frankel, Oblimersen Bcl-2: facilitating apoptosis in anticancer treatment, *Antisense Nucleic Acid Drug Dev.* 2002, 12, 193-213.
34. K. Nakayawa, K. Yamamura, S. Maeda, M. Ichihashi, Bcl-2 expression in epidermal keratinocytic diseases. *Cancer* 1994, 74, 1720-1724.
35. J.R. John Jr, N. Stephen, J.S. Thomas, Murine susceptibility to two-stage skin carcinogenesis is influenced by the agent used for promotion, *Carcinogenesis* 1984, 5, 301-307.

36. X. Zhang, V. Kundoor, S. Khalifa, D. Zeman, H. Fahmy, C. Dwivedi, Chemopreventive effects of sarcophine-diol on skin tumor development in CD-1 mice, *Cancer Lett.* 2007, 253, 53-59.
37. V. V. Venuganti, O. Perumal, Poly(amidoamine) dendrimers as skin penetration enhancers: Influence of charge, generation and concentration. *J. Pharm. Sci.* 2009, 98, 2345-2356.
38. V.V. Venuganti, Dendrimer based nanocarriers for transcutaneous drug delivery. *Ph.D. Dissertation,* South Dakota State University, 2010.
39. R. Alvarez-Roman, A. Naik, Y.N.Kalia, H. Fessi, R.H. Guy, Visualization of skin penetration using confocal laser scanning microscopy. *Eur. J. Pharm. Biopharm.* 2004, 58, 301-316.
40. R.H. Guy, Y.N. Kalia, M.B. Delgado-Charro, V. Merino, A. Lopez, D. Marro, Iontophoresis: electrorepulsion and electroosmosis, *J. Control. Release* 2000, 64, 129-132.
41. U. Jacobi, M. Kaiser, R. Toll, S. Mayelsdory, H. Audring, N. Otberg, W. Stacy, J. Lademan, Porcine ear skin: an in vitro model for human skin. *Skin. Res. Technol.* 2007, 13, 19-24.
42. R. DeLong, K. Stephenson, T. Loftus, M. Fisher, S. Alahari, A. Nolting, R.L. Juliano, Characterization of complexes of oligonucleotides with polyamidoamine starburst dendrimers and effects on intracellular delivery, *J. Pharm. Sci.* 1997, 86, 762-764.
43. C.M.J. Tilli, M.A.M.V. Steensel, G.A.M. Krekels, H.A.M. Neumann, F.C.S. Ramaekers, Molecular aetiology and pathogenesis of basal cell carcinoma, *Br. J. Dermatol.* 2005, 152, 1108-1124.
44. M.R. Hussein, Z.H. Al-Badaiwy, M.N. Guirguis, Analysis of p53 and bcl-2 protein expression in the non-tumorigenic, pretumorigenic, and tumorigenic keratinocytic hyperproliferative lesions, *J. Cutan. Pathol.* 2004, 31, 643-651.
45. B. Jansen, H.S. Wadl, B. Jansen, H. Schlagbauer-Wadl, B.D. Brown, R.N. Bryan, A. van Elsas, M. Muller, K. Wolff, H.G. Eichler, H. Pehamberger, Bcl-2 antisense therapy chemosensitizes human melanoma in SCID mice, *Nat. Med.* 1998, 4, 232-234.
46. R.K. Boutwell, Some biological aspects of skin carcinogenesis, *Prog. Exp. Tumor Res.* 1984, 4, 207-250.
47. J. DiGiovanni, T.J. Slaga, R.K. Bowtwell, Comparison of the tumor-initiating activity of 7, 12-dimethylbenzanthracene and benzopyrene in female SENCAR and CD-1 mice, *Carcinogenesis* 1980, 1, 381-389.

48. M. Chen, M. Zakrewsky, V. Gupta, A.C. Anselmo, D.H. Slee, J.A. Muraski, S. Mitragotri, Topical delivery of siRNA into skin using SPACE-peptide carriers, *J. Control. Release* 2014, 179, 33–41.

49. K. Kigasawa, K. Kajimoto, T. Nakamura, S. Hama, K. Kanamura, H. Harashima, K. Kogure, Noninvasive and efficient transdermal delivery of CpG-oligodeoxynucleotide for cancer immunotherapy, *J. Control. Release* 2011, 150, 256-265.

**Table 1**. Particle size and zeta potential of Dendrimer-ASO complexes

| Complex (N/P ratio) | Size (nm) * | PDI | Zeta Potential (mv) |
|---|---|---|---|
| Dendrimer-ASO (1:10) | 150 ± 12 | 0.4 ± 0.1 | -42 ± 6 |
| Dendrimer-ASO (1:1) | 123 ± 18 | 0.3 ± 0.02 | -11 ± 2 |
| Dendrimer-ASO (10:1) | 84 ± 20 | 0.2 ± 0.04 | +9 ± 0.9 |

PDI – polydispersity index; * Values are shown as mean ± SD, n=3

**Table 2**. Percent of total pixels from ASO-nanocarrier complexes within the viable epidermis after passive and iontophoretic delivery.

| Complex | Passive delivery (%) | Iontophoresis (%) | ER |
|---|---|---|---|
| Free ASO | 5.8 ± 2.1 | 10.1 ± 3.2 | 1.7 |
| ASO-dendrimer complex | 10.1 ± 3.3 | 50.5 ± 13.6 [ab] | 5.0 |

ER represents enhancement ratio and was calculated by dividing percent of total pixels from iontophoresis with that of passive delivery. Values represent percent of pixels from the viable epidermis in comparison to the total pixel from 0-100 µm. Stratum corneum thickness was considered 20 µm and viable epidermis was considered to be from 20 to 100 µm.[31] Values are presented as mean ± SD, n=4. 'a' represents that the value is significantly different compared to respective passive delivery and 'b' represents that the value is significantly different compared to iontophoretic delivery of free ASO at $P < 0.05$.

**Figure Legends:**

**Fig. 1**. I*n vivo* iontophoretic set up. Agarose gel (0.3%) containing ASO-dendrimer complex was placed on a tumor and control electrode was placed on the normal skin.

**Fig. 2**. CLSM images of porcine skin after passive (upper panel) and iontophoretic delivery (lower panel; 0.3 mA/cm$^2$) of ASO-dendrimer complexes for 4 hrs. Optical sections were taken in *xz*-plane from surface to 100 µm depth at 1µm step size and 40*x* magnification. Vertical bar represents 20 µm.

**Fig. 3**. Colocalization of dendrimer (green channel; FITC labeled) and ASO (red channel; rhodamine labeled) after 4 hrs passive (top panel) and iontophoretic delivery (0.3 mA/cm$^2$; lower panel) ASO-dendrimer complex through porcine skin. Images are cumulative of 22 optical sections taken from surface to 100 µm depth in *xyz* plane (i) and in *xz* plane (ii). Vertical bar represents 20 µm.

**Fig. 4**. Flow cytometric analysis of A431 cells after incubation with free ASO (a) and ASO-dendrimer complex (b) for different time periods. The shift in fluorescence intensity as a function of treatment time is shown in the figure

**Fig. 5**. Effect of treatment on tumor volume. The treatment was carried out at days 1, 3, 5 and 7. The y-axis represents the tumor volume at the end of day-7 compared to the initial tumor volume at day 0 (%). *represents that the value is significantly different compared to all other groups at $p<0.05$. id – intradermal administration; P – passive deliver, IP- iontophoretic delivery, ASO- anti-sense oligonucleotide, SO- sense oligonucleotide. The relative tumor volume was calculated by comparing the tumor volume at the end of 7-day treatment to the tumor volume at day 0 before starting the treatment (i.e. % of initial tumor volume). Each value represents mean ± SD (n=3-5).

**Fig. 6**. Bcl-2 protein expression in skin tumor after treatment with ASO. (A) Bcl-2 and β-actin protein bands from Western blot. (B) Relative intensity of Bcl-2 band with respect to the control β-actin band in skin tumor after different treatments. The band intensity was determined by densitometric analysis and the values represent the ratio of Bcl-2 band intensity and β-actin band intensity. Each value represents mean ± SD (n=3). *represents that the value is significantly different compared to all the other groups at $p<0.05$. id – intradermal administration; P- passive application; IP – iontophoresis, ASO- anti-sense oligonucleotide, SO- sense oligonucleotide. 1, saline-id; 2, SO-dendrimer-id; 3, ASO-id; 4, ASO-dendrimer-id; 5, ASO-P; 6, ASO-IP; 7, ASO-dendrimer-P; 8, ASO-dendrimer-IP.

**Fig. 7**. TUNEL assay (fluorescein labeled) was performed on cryosections (8 µm thickness) of skin tumor after different treatments. Positive control was treated with DNase I to induce nicks in the DNA. Arrows and arrow heads indicate apoptotic cells in the epidermis and follicular cells. The red fluorescence is nuclear staining with propidium iodide (PI). ASO- anti-sense oligonucleotide; IP-iontophoresis, dUTP- deoxynucleotidyl transferase.

**Figure 1**

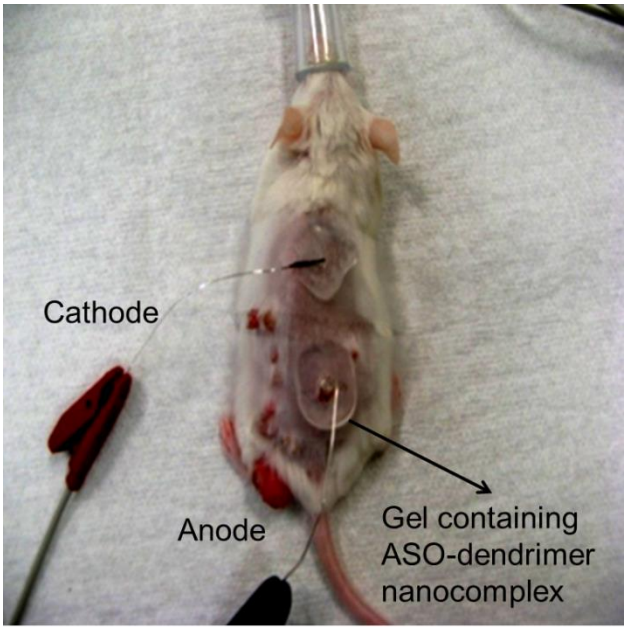

**Figure 2**

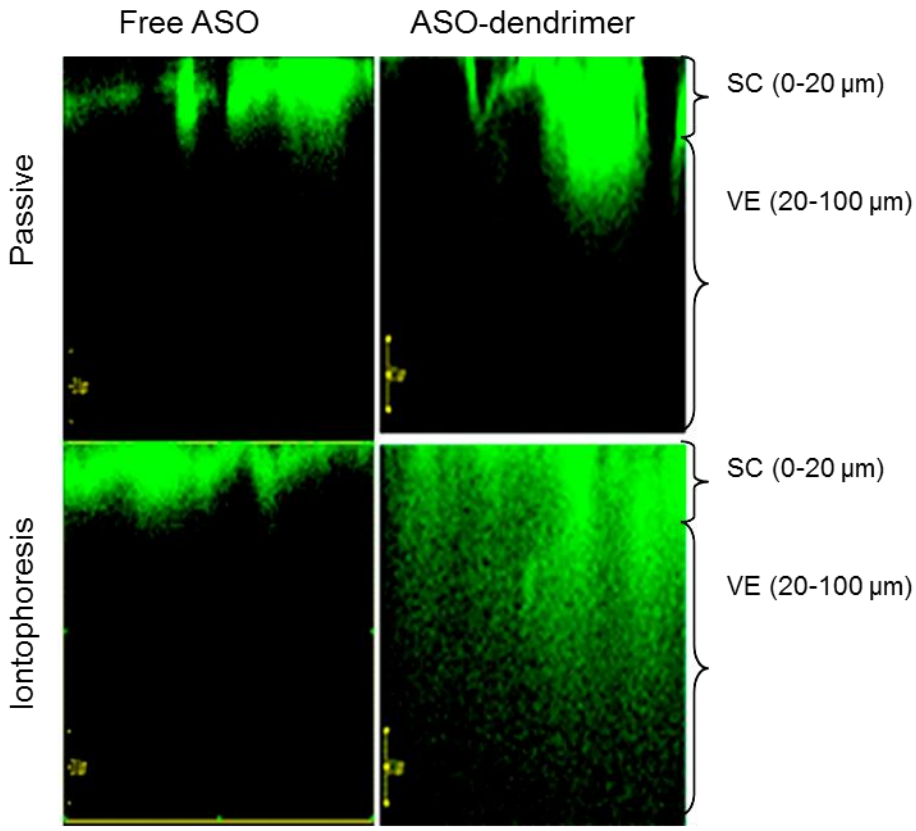

**Figure 3**

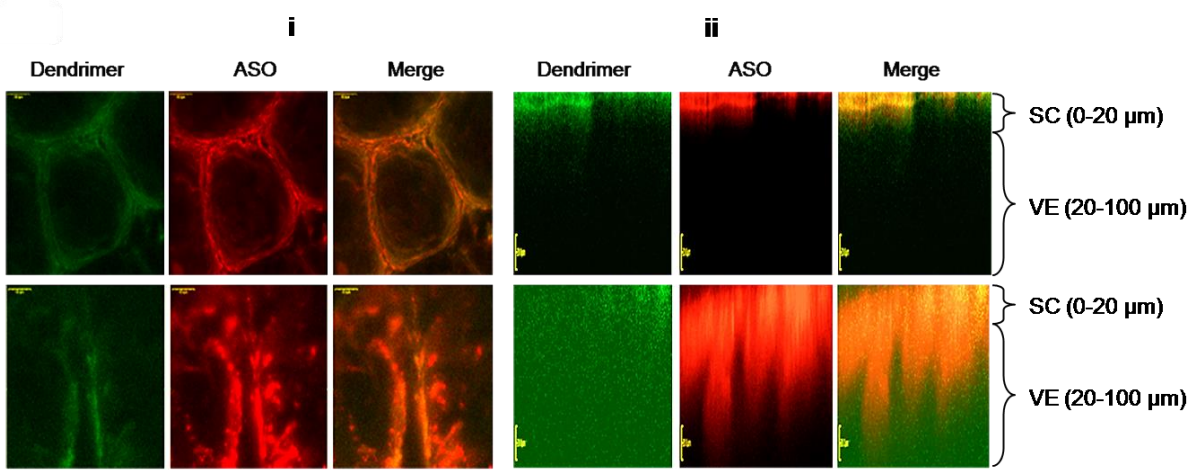

**Figure 4**

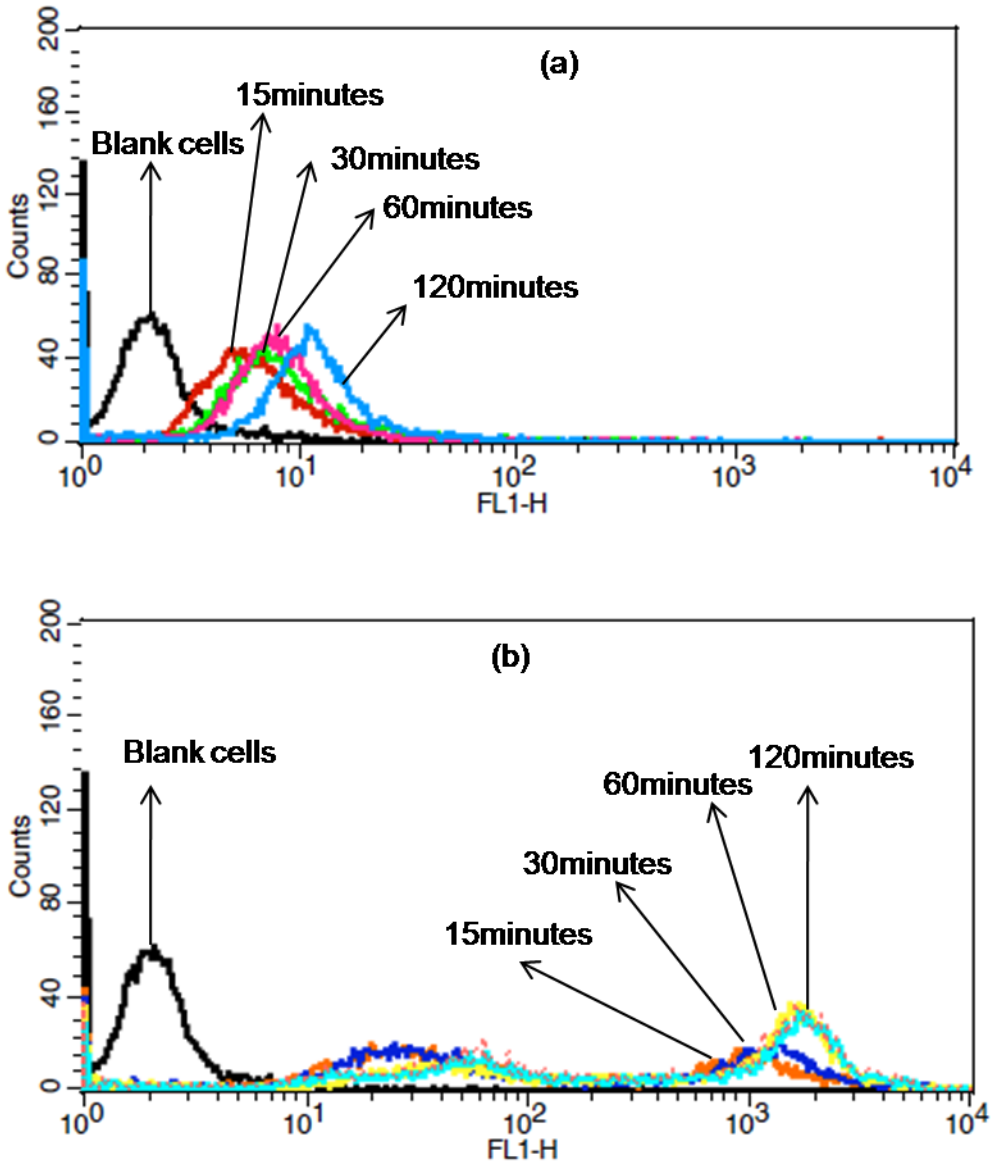

**Figure 5**

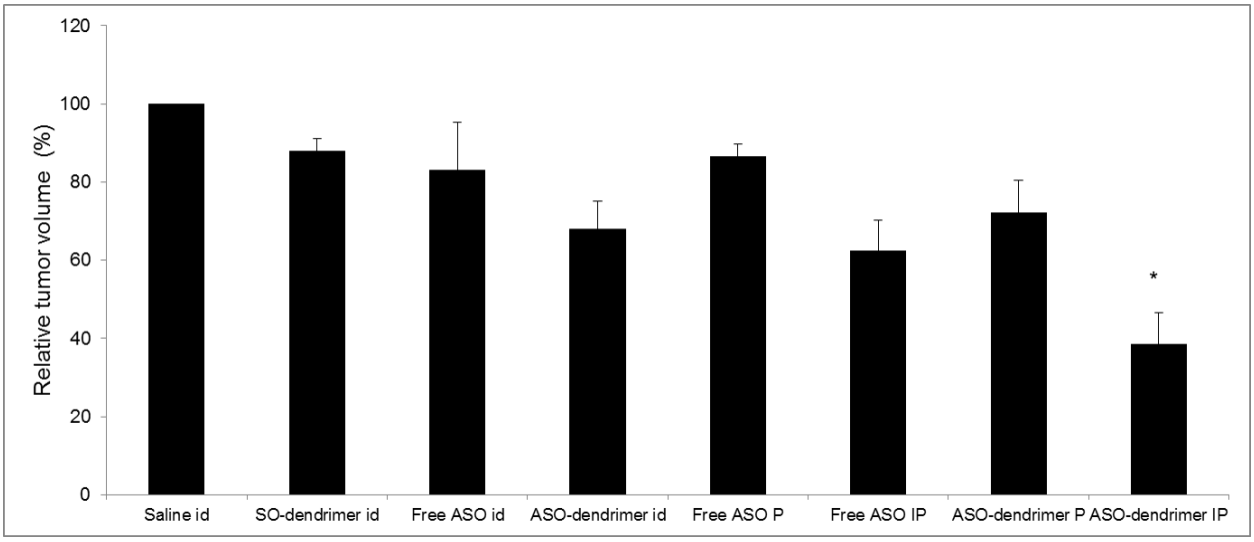

**Figure 6**

A.

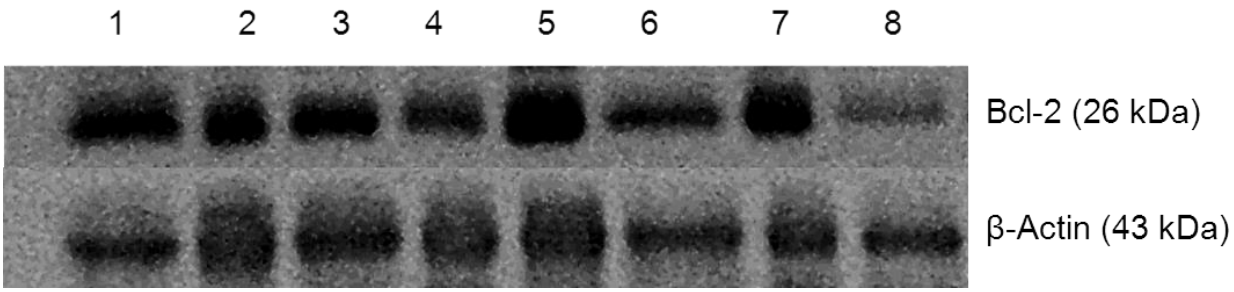


B.

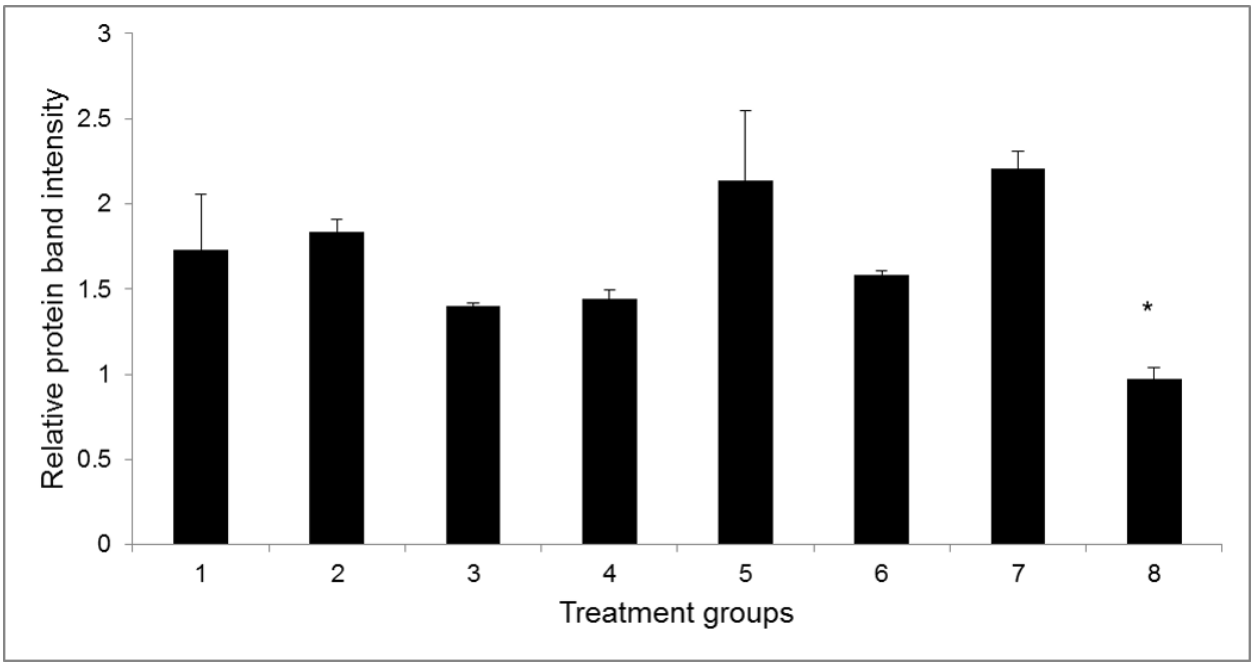

**Figure 7**